Evaporation induced wrinkling of graphene oxide at the nanoparticle interface

Feng Wang and Juewen Liu*

Department of Chemistry, Waterloo Institute for Nanotechnology, University of Waterloo, Waterloo, ON, N2L 3G1, Canada

Email: liujw@uwaterloo.ca

With the thickness of only a single atomic layer, graphene displays many interesting surface properties. A general observation is that wrinkles are formed on graphene oxide (GO) when it is dried in the presence of adsorbed inorganic nanoparticles. In this case, evaporation induced wrinkling is not an elastic deformation but is permanent. Understanding the nanoscale force of wrinkle formation is important for device fabrication and sensing. Herein, we employ surface functionalized gold nanoparticles (AuNPs) as a model system. All tested AuNPs induced wrinkling, including those capped by DNA, polymers and proteins. The size of AuNPs is less important compared to the property of solvent. Wrinkle formation is attributed to drying related capillary force acting on the GO surface, and a quantitative equation is derived. After drying, the adsorption affinity between GO and AuNPs is increased due to increased contact area.

Surface forces at the solid/liquid/gas interface govern many fundamental and interesting phenomena in nanotechnology, soft materials science, and self-assembly.[1-4] For example, evaporation-induced self-assembly (EISA) takes advantage of the capillary force on nanoparticles,[5,6] while selective wetting of inverse opal films allows liquid identification.[7] Most of the previous work was carried out on a hard solid surface and the solid substrate deformation was rarely explored. We reason that new hybrid materials and their assembly may be produced by such deformation.

Graphene is a single layer of graphite.[8] While graphene is mechanically strong,[9,10] its atomic scale thickness might allow its deformation with surface forces. In the past decade, graphene has been interfaced with various inorganic nanoparticles to form functional hybrid materials with unique catalytic, magnetic, and optical properties.[11-19] While direct chemical bonding is possible,[20] many of these materials are fabricated via solution routes, where inorganic nanoparticles are adsorbed by the graphene oxide (GO) in an aqueous solution.[21,22] Then the sample is dried for further characterization or application. An example is shown in Figure 1, where gold nanoparticles (AuNPs) are adsorbed by GO. As the solvent evaporates, a meniscus is formed at the interface, exerting an attractive force between the AuNP and GO. In this work, we aim to use polymer-functionalized AuNPs and GO as a model system to study the drying effect and the resulting changes on the GO surface.

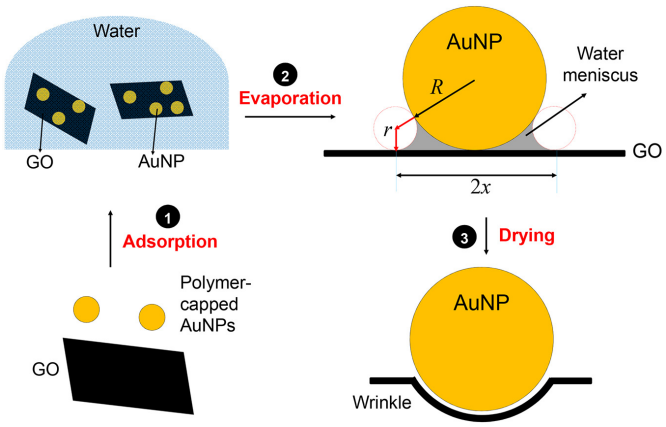

Figure 1. Schematics of evaporation induced meniscus formation at the AuNP/GO interface and capillary force analysis. Step 1: AuNP adsorption by GO. Step 2: meniscus formation at the interface. The radius of the AuNP is *R*, the radium of the meniscus is *r*, and the radius of the water at the interface is *x*. Step 3: upon drying, a wrinkle is induced wrapping around the AuNP and increasing adsorption strength.

We chose AuNPs since its surface property and size can be readily controlled. Its high electron density also makes microscopic imaging easy. In addition, composite materials made of AuNPs and GO are useful for making biosensors and catalysis.[23-25] We prepared 13 nm AuNPs capped by thiolated T_{15} DNA (i.e. an oligonucleotide with 15 thymines) and mixed it with GO. When the sample was dried and imaged by TEM, almost all the AuNPs are associated with wrinkles on GO (Figure 2A). The ones that are not associated with wrinkles are marked by the while circles. By counting at least 300 AuNPs from different GO sheets, we showed the statistics in Figure 3A (the last bar). Similar observations were made with 13 nm AuNPs capped with A_{15} (Figure 2B) and for 5 nm AuNPs capped with A_{15} (Figure 2C). While poly-T DNA binds to GO relatively weakly and poly-A binds strongly,[26-28] AuNP associated wrinkling was observed in both cases. For comparison, the original citrate capped AuNPs are not

adsorbed by GO (Figure S1), and cannot be directly used for this study.

Similar observations were made with AuNPs capped by branched polyethylenimine (BPEI, Figure 2D) and bovine serum albumin (BSA, Figure 2E). BPEI is a cationic polymer considered to be one of the most efficient gene transfer vectors,[29] and BSA is a common protein. By searching the literature, we found that many other nanoparticles produced wrinkles on GO as well.[13,30-34] Our own experiment also indicated that silica nanoparticles can produce very obvious wrinkling (Figure S2A). On the other hand, if GO is dried by itself, no extensive wrinkling was observed (Figure 2F). This indicates that wrinkling is produced due to the presence of nanoparticles. Since these different polymers with different properties all produced a similar effect, it suggests that the reason might not relate to the specific chemical property of the capping agents.

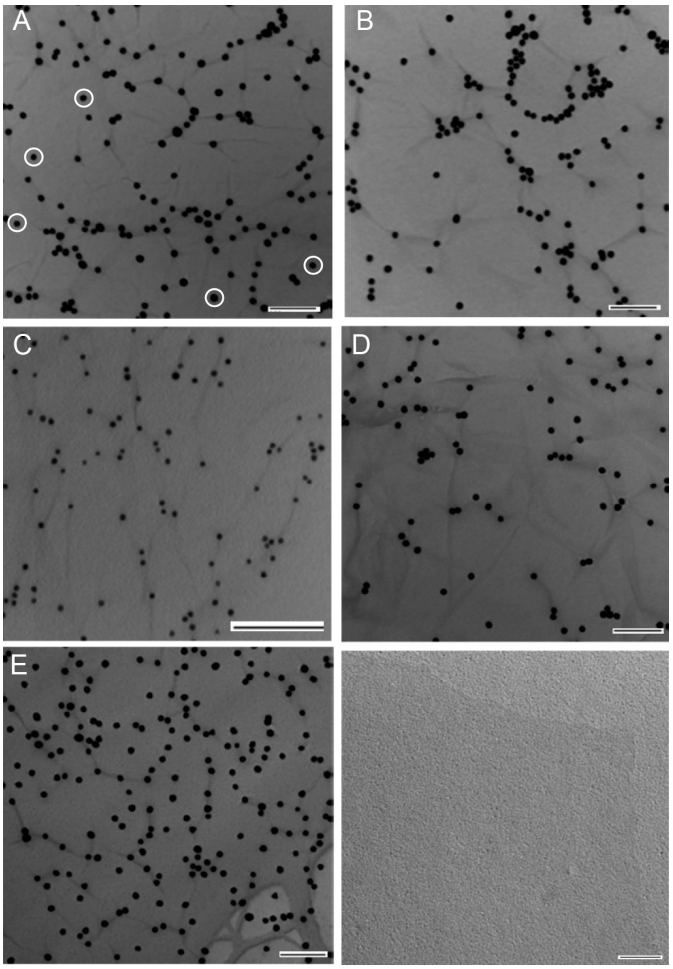

Figure 2. TEM images of (A) GO-AuNP/HS-T_{15} (13 nm), (B) GO-AuNP/HS-A_{15} (13 nm), (C) GO-AuNP/HS-A_{15} (5 nm), (D) GO-AuNP/BPEI (12 nm), (E) GO-AuNP/BSA (13 nm), and (F) free GO sheets (no AuNPs). Scale bar = 100 nm in all the micrographs. The circles in (A) indicate AuNPs that are not associated with wrinkles as observed by TEM.

We reason that hydrophilicity is the common property of all these capping agents. An attractive capillary force is formed at the AuNP and GO interface due to the water meniscus as indicated in Figure 1. GO can be locally deformed by this force, producing the wrinkles. The wrinkling has a line or spiked shape in most cases and the AuNPs are sitting in the middle or ends of the line or at the center of the spikes. This suggests that each AuNP can exert a long-ranged stress on the GO surface.

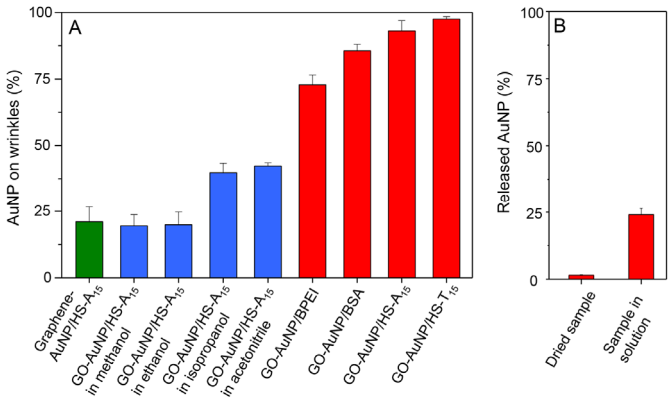

Figure 3. (A) Quantification of the percentage of various AuNPs (13 nm) sitting on wrinkles based on the TEM results. (B) Percentage of AuNP/HS-A_{15} (13 nm) release by 4 M urea for the dried sample and the original always hydrated sample. Dried sample released less indicating tighter binding.

To test our hypothesis, we designed the following experiments. First, A_{15}-capped AuNPs were mixed with GO to achieve adsorption. Then KCN was added to the dispersion before drying (Figure 4A). In this case, we did not observe much wrinkling and barely any AuNPs were observed, since they were dissolved by KCN. This experiment indicates that wrinkles are formed during drying instead of in solution. In another experiment, the sample was dried first and then soaked in KCN solution to dissolve the AuNPs. After drying again, we still observed extensive wrinkling (Figure 4B), indicating that once formed, the wrinkles would remain even after removal of AuNPs. Therefore, evaporation induced wrinkling is not an elastic deformation but is permanent.

The scheme on the right side of Figure 1 is an interesting model of the solid/liquid/air interface. To explain wrinkle formation, a force analysis is performed. Considering a AuNP (radius = R) drying on a GO surface, a water meniscus (water surface tension = γ; meniscus radius of curvature = r) is formed at the interface at the late stage of drying. Due to the hydrophilic nature of both AuNP and GO, the meniscus should have the shape drawn in Figure 1, where the radius of the water stain on GO is x. From simple geometry, we can write $x^2 \cong 4rR$ (see Figure S3 for detail). Therefore, the Laplace pressure is $\Delta P = 2\gamma/r = 8\gamma R/x^2$. The Laplace pressure is the pressure difference at the water interface to account for the curved meniscus surface. If the contact area is A, the amount of force on GO is $F = \Delta P \cdot A = (8\gamma R/x^2)(\pi x^2) = 8\pi\gamma R_p$. This means that the force is quite uniform during the drying process and is not related to the contacting area of the remaining water stain. It is only related to the particle size and the surface tension of the solvent. Give the size of a 13 nm AuNP with R = 6.5 nm, the force F = 11.8 nN.

GO deformation was measured using an AFM tip, where even 2 nN caused significant deformation.[35] In that case, the size of the AFM tip was 23.9 nm, which is larger than our AuNPs. In this regard, the pressure applied on GO is even greater in our system. This

comparison has rationalized the possibility of GO wrinkle formation upon drying.

Based on the above equation and analysis, we next aim to rationally control the drying process. First, the attractive force is related to the size of AuNPs. When we reduced the size of AuNPs from 13 nm to 5 nm, a similar wrinkling effect was observed (Figure 2C), suggesting that the force is still strong enough even after decreasing it by 2.6-fold. Next we tried ethanol, which is a lower surface tension solvent (Figure 4C). Interestingly, no extensive wrinkles were observed and most of the AuNPs were not associated with wrinkles either (Figure 3A, the blue bar for quantification). The surface tension of ethanol is only ~3-fold lower than that of water. Since using the 5 nm AuNPs still induced wrinkling in water, this decreased surface tension alone cannot explain the lack of wrinkling with ethanol. We reason that the rate of evaporation might also be important. Ethanol evaporates much faster and the time for the capillary force action might be much shorter. Ethanol is not a good solvent for DNA either, and this might also apply a less attractive force (e.g. by increasing the contact angle). We further tested a few other organic solvents, including methanol, isopropanol, and acetonitrile, all showing decreased extent of AuNP-associated wrinkling (Figure S2). All the tested alcohols have similar surface tension (differ only by ~5%), but it is interesting to note that isopropanol has more wrinkling than the other two. This may be attributed to its slower evaporation rate.

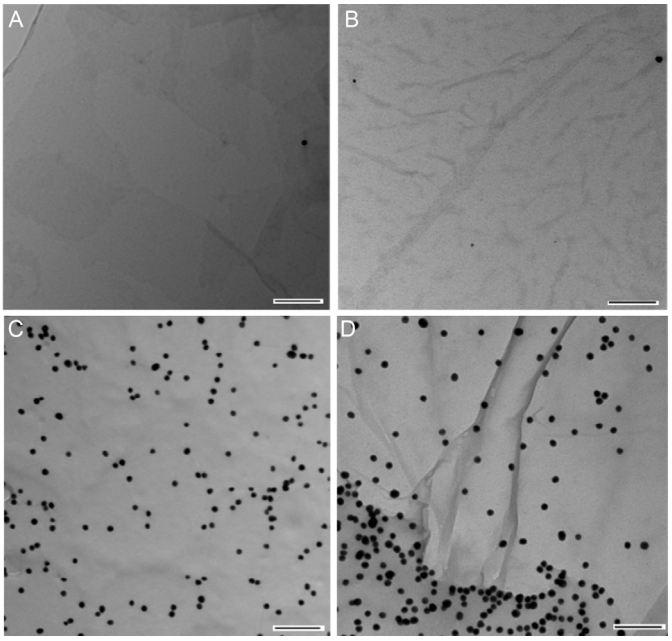

Figure 4. TEM images of (A) GO-AuNP/HS-A_{15} (13 nm) treated with 5 mM KCN after mixing AuNP with GO. Then the sample was dried. Little wrinkling was observed. (B) GO-AuNP/HS-A_{15} (13 nm) dried on the grid first, and then treated with 5 mM KCN. Scale bar = 100 nm. TEM image of (C) drying of GO-AuNP/HS-A_{15} (13 nm) when dispersed in ethanol, (D) drying graphene-AuNP/HS-A_{15} (13 nm) in water. Note that in (D) the AuNPs are adsorbed on pristine graphene instead of GO. Scale bar = 100 nm for all the micrographs.

Finally, we changed the substrate from GO to pristine graphene. GO is hydrophilic due to its rich oxygenated groups and its water contact angle is reported to be ~67°.[36] Although freshly cleaved graphene was reported to be hydrophilic (contact angle smaller than 90°),[37] our graphene was made by chemical reduction and has been exposed to air for a long time. Therefore, it should be hydrophobic. Indeed, we failed to see the association of AuNPs with wrinkles (Figure 4D). Although there are a lot of wrinkles on pristine graphene, they do not overlap with AuNPs, indicating the AuNPs were not responsible for the wrinkles. Pristine graphene is known to form wrinkles when in contact with water, and this type of wrinkling is not the focus of the current study. We are dealing with the permanent wrinkles from drying in the presence of nanoparticles. When the water contact angle is greater than 90°, the capillary force becomes repulsive, thus pushing the AuNPs away from the graphene surface during drying. Note that the molecular interaction between the DNA on the AuNPs and graphene is still attractive, which is responsible for a high density of AuNPs on graphene. Only the capillary force induced by the water meniscus became repulsive. Taken together, the interfacial interaction on GO can be controlled by tuning the capillary force.

This fundamental interfacial analysis has increased our understanding on this important system, which may be useful for controlling the property the resulting materials. For example, from the above analysis, the contact area between AuNP and GO should increase upon wrinkle formation. Originally, there is only a single contact point. After drying, the contact area also includes the wrinkle that wraps around AuNPs, which forms a 3D binding pocket (Figure 1). To test whether binding is indeed tighter, we treated the dried and hydrated AuNP/GO complexes with 4 M urea. Since the AuNPs are attached to GO by DNA, urea can wash away the hydrogen bonding responsible for this binding.[38] We did not observe any release of AuNPs for the dried sample, but for the hydrated sample, ~20% of the AuNPs were released (Figure 3B), confirming that the AuNPs were more stably adsorbed after drying.

Wrinkles are observed in GO even in the absence of AuNPs. Those wrinkles are attributed to defects in the carbon structure due to epoxy groups and the subsequent release of CO_2, leaving behind defect vacancies as weak points.[39] Since epoxy groups imply strains, the GO sheet may kink to form an energetically more favorable configuration, especially when several epoxy groups stack. Apparently, during drying in the presence of adsorbed AuNPs, the amount of wrinkle increased. These wrinkles are not confined just at the site of adsorption, but rather can extend tens of nanometers. Since GO is composed of nanoscale domains of highly oxidized regions dispersed in more carbon rich domain, we reason that wrinkles are induced along the defects with weaker mechanical strength. Therefore, by observing the wrinkling pattern, we may extract information about the distribution of defects on GO, which will be a topic of subsequent studies.

Conclusions

In summary, we performed a careful force analysis at the AuNP/GO interface during drying. The capillary force is strong enough to deform GO locally to cause wrinkle formation. The wrinkling in turn makes binding of AuNPs even more strongly due the new 3D binding pocket. This study provides important insights into the interface science of GO, and it will be useful for understanding the surface chemistry and reaction mechanisms related to GO and other nanomaterials.

Acknowledgement.

Funding for this work is from the University of Waterloo, the Canadian Foundation for Innovation, the NSERC of Canada, and the

Early Researcher Award from the Ontario Ministry of Research and Innovation.

Notes and references

[a] *Department of Chemistry, Waterloo Institute for Nanotechnology, University of Waterloo, Waterloo, Ontario, N2L 3G1, Canada. Fax: 519 7460435; Tel: 519 8884567 Ext. 38919; E-mail: liujw@uwaterloo.ca.*

Electronic Supplementary Information (ESI) available: [methods]. See DOI: 10.1039/c000000x/

1. Y. Gao and Z. Tang, *Small*, 2011, **7**, 2133-2146.
2. K. J. M. Bishop, C. E. Wilmer, S. Soh and B. A. Grzybowski, *Small*, 2009, **5**, 1600-1630.
3. W. Cheng, N. Park, M. T. Walter, M. R. Hartman and D. Luo, *Nat Nano*, 2008, **3**, 682-690.
4. J. N. Israelachvili, *Intermolecular and Surface Forces, Third Edition: Revised Third Edition*, Academic Press, New York, 2011.
5. C. J. Brinker, Y. F. Lu, A. Sellinger and H. Y. Fan, *Adv. Mater.*, 1999, **11**, 579-+.
6. Y. F. Lu, H. Y. Fan, A. Stump, T. L. Ward, T. Rieker and C. J. Brinker, *Nature*, 1999, **398**, 223-226.
7. I. B. Burgess, L. Mishchenko, B. D. Hatton, M. Kolle, M. Lončar and J. Aizenberg, *J. Am. Chem. Soc.*, 2011, **133**, 12430-12432.
8. A. K. Geim, *Science*, 2009, **324**, 1530-1534.
9. M. A. Rafiee, J. Rafiee, Z. Wang, H. H. Song, Z. Z. Yu and N. Koratkar, *Acs Nano*, 2009, **3**, 3884-3890.
10. D. A. Dikin, S. Stankovich, E. J. Zimney, R. D. Piner, G. H. B. Dommett, G. Evmenenko, S. T. Nguyen and R. S. Ruoff, *Nature*, 2007, **448**, 457-460.
11. K. Yang, L. Feng, X. Shi and Z. Liu, *Chem. Soc. Rev.*, 2013, **42**, 530-547.
12. C. S. Wang, J. Y. Li, C. Amatore, Y. Chen, H. Jiang and X. M. Wang, *Angew. Chem. Int. Ed.*, 2011, **50**, 11644-11648.
13. J. Liu, S. Fu, B. Yuan, Y. Li and Z. Deng, *J. Am. Chem. Soc.*, 2010, **132**, 7279-7281.
14. L. H. Tang, Y. Wang, Y. Liu and J. H. Li, *ACS Nano*, 2011, **5**, 3817-3822.
15. I. V. Lightcap and P. V. Kamat, *J. Am. Chem. Soc.*, 2012, **134**, 7109-7116.
16. G. M. Scheuermann, L. Rumi, P. Steurer, W. Bannwarth and R. Muelhaupt, *J. Am. Chem. Soc.*, 2009, **131**, 8262-8270.
17. W. B. Hu, C. Peng, M. Lv, X. M. Li, Y. J. Zhang, N. Chen, C. H. Fan and Q. Huang, *Acs Nano*, 2011, **5**, 3693-3700.
18. I. Ocsoy, B. Gulbakan, T. Chen, G. Zhu, Z. Chen, M. M. Sari, L. Peng, X. Xiong, X. Fang and W. Tan, *Adv. Mater.*, 2013, **25**, 2319–2325.
19. Z.-L. Song, X.-H. Zhao, W.-N. Liu, D. Ding, X. Bian, H. Liang, X.-B. Zhang, Z. Chen and W. Tan, *Small*, 2013, **9**, 951-957.
20. G. Goncalves, P. A. A. P. Marques, C. M. Granadeiro, H. I. S. Nogueira, M. K. Singh and J. Grácio, *Chem. Mater.*, 2009, **21**, 4796-4802.
21. Y. Li and Y. Wu, *J. Am. Chem. Soc.*, 2009, **131**, 5851-5857.
22. F. Chen, S. Liu, J. Shen, L. Wei, A. Liu, M. B. Chan-Park and Y. Chen, *Langmuir*, 2011, **27**, 9174-9181.
23. S. P. Song, Y. Qin, Y. He, Q. Huang, C. H. Fan and H. Y. Chen, *Chem. Soc. Rev.*, 2010, **39**, 4234-4243.
24. H. Wang, R. H. Yang, L. Yang and W. H. Tan, *ACS Nano*, 2009, **3**, 2451-2460.
25. S. Mao, G. H. Lu, K. H. Yu, Z. Bo and J. H. Chen, *Adv. Mater.*, 2010, **22**, 3521-+.
26. B. Liu, Z. Sun, X. Zhang and J. Liu, *Anal. Chem.*, 2013, **85**, 7987-7993.
27. A. K. Manna and S. K. Pati, *J. Mater. Chem. B*, 2013, **1**, 91-100.
28. N. Varghese, U. Mogera, A. Govindaraj, A. Das, P. K. Maiti, A. K. Sood and C. N. R. Rao, *ChemPhysChem*, 2009, **10**, 206-210.
29. U. Lungwitz, M. Breunig, T. Blunk and A. Göpferich, *Eur. J. Pharm. Biopharm.*, 2005, **60**, 247-266.
30. S. Salgado, L. Pu and V. Maheshwari, *The Journal of Physical Chemistry C*, 2012, **116**, 12124-12130.
31. J. Luo, X. Zhao, J. Wu, H. D. Jang, H. H. Kung and J. Huang, *The Journal of Physical Chemistry Letters*, 2012, **3**, 1824-1829.
32. W.-N. Wang, Y. Jiang and P. Biswas, *The Journal of Physical Chemistry Letters*, 2012, **3**, 3228-3233.
33. S. U. Yu, B. Park, Y. Cho, S. Hyun, J. K. Kim and K. S. Kim, *Acs Nano*, 2014, **8**, 8662-8668.
34. L. A. L. Tang, W. C. Lee, H. Shi, E. Y. L. Wong, A. Sadovoy, S. Gorelik, J. Hobley, C. T. Lim and K. P. Loh, *Small*, 2012, **8**, 423-431.
35. J. W. Suk, R. D. Piner, J. An and R. S. Ruoff, *Acs Nano*, 2010, **4**, 6557-6564.
36. S. Wang, Y. Zhang, N. Abidi and L. Cabrales, *Langmuir*, 2009, **25**, 11078-11081.
37. Z. T. Li, Y. J. Wang, A. Kozbial, G. Shenoy, F. Zhou, R. McGinley, P. Ireland, B. Morganstein, A. Kunkel, S. P. Surwade, L. Li and H. T. Liu, *Nat. Mater.*, 2013, **12**, 925-931.
38. J. S. Park, H.-K. Na, D.-H. Min and D.-E. Kim, *Analyst*, 2013, **138**, 1745-1749.
39. H. C. Schniepp, J.-L. Li, M. J. McAllister, H. Sai, M. Herrera-Alonso, D. H. Adamson, R. K. Prud'homme, R. Car, D. A. Saville and I. A. Aksay, *J. Phys. Chem. B*, 2006, **110**, 8535-8539.